

Larval performance, osteological development and skeletal abnormalities in wreckfish (*Polyprion americanus*) under a standard rearing protocol and different light intensities and rearing temperatures

Amin Mokhles Abadi Farahani^{a,b}, Maximo Coronado^c, Santiago Bragado^a, Maria José Justo^a, Xoana Blanco^a, Aitor Sotelo^a, Paola Navarrete^c, Blanca Álvarez-Blázquez^a, Ignacio Fernández^{a,*}

^a Centro Oceanográfico de Vigo, Instituto Español de Oceanografía (IEO), CSIC, 36390 Vigo, Spain.

^b Department of Natural Resources (Fisheries Division), Isfahan University of Technology (IUT), 8415683111 Isfahan, Iran

^c Laboratorio de Microbiología y Probióticos, Instituto de Nutrición y tecnología de los Alimentos (INTA), Universidad de Chile, El Líbano 5524, Macul, Chile

ARTICLE INFO

Keywords:

Skeletogenesis
Deformity
Light intensity
Water temperature
Incubation

ABSTRACT

Wreckfish (*Polyprion americanus*) is a promising new species for aquaculture diversification due to its fast growth, late reproductive maturation, and high market price. Nowadays, low larval survival is considered the biggest limitation in wreckfish farming. Here, the fertilization, hatching and survival rates of 20 spawning events from an established wreckfish broodstock have been analyzed in order to characterize the main bottlenecks in wreckfish early and larval development. The ontogenesis of the skeletal system and the incidence of skeletal deformities have been assessed in 632 samples from larval rearing trials using currently available protocols. Furthermore, the effect of different rearing temperatures (13 vs 16 °C) and light intensities at water surface (600, 900 and 1200 lx) on the skeletal development have been also explored. Results showed as while a variable egg fertilization rate (61.75 ± 34.62%) were achieved, a very poor hatching (4.52 ± 9.27%) and survival rate (0.01 ± 0.00%) until 71 days post hatching (dph) were observed. Swim bladder inflation was first seen at 7 dph, and at 11 and 25 dph a 61–63% of fish functional swim bladder. The first skeletal structures to be formed were those related with breathing and feeding activities (e.g., cleithrum, Meckel's cartilage and ceratobranchials) and were visible in larvae of 4–5 mm of standard length (SL). Ossification of the vertebral column progressed in an anterior-to-posterior direction, being fully ossified at 7–14 mm of SL. Regarding the skeletal deformities, a high incidence (63%) of jaw deformity (particularly lower jaw deformity) was observed in larvae of 4–5 mm of SL, progressively decreasing (up to 5%) in larvae of >6 mm of SL. Deformed vertebrae (compressed, fused, and/or displaced) were mainly located at 13 to 15th vertebra, and were associated to lordosis, most probably due to the no swim bladder inflation. No clear relationship between temperature and the incidence of lower jaw deformity was observed during endotrophic larval development. Light intensity had a clear effect on survival but not in skeletal development. Larvae reared under 600 lx had lower survival (0.15 ± 0.21%) at 21 dph than when reared with 900 and 1200 lx (0.6 ± 0.28 and 0.7 ± 0.28%, respectively). The present research work represents an important step forward to solve wreckfish larval rearing bottlenecks, suggesting that while temperature and light intensity might have an effect on wreckfish larval survival and development, egg quality and incubation seemed to be the most limiting factors for successful wreckfish aquaculture.

1. Introduction

Wreckfish (*Polyprion americanus*) is a pan oceanic marine deep-water fish able to reach a size of 100 kg (Deudero and Morales-Nin, 2000; Sedberry et al., 1999), but declared as Near Threatened by the IUCN

(Collette et al., 2015). Recently, it has been proposed as an interesting new species for aquaculture diversification in Europe based on species-specific features (Pérez et al., 2019). Wreckfish has: i) fast growth, reaching 2.0 and 5.0 kg in 12 and 24 months, respectively (Papanoulakis et al., 2004); ii) potentially good feed conversion rates (as low

* Corresponding author.

E-mail address: Ignacio.fernandez@ieo.csic.es (I. Fernández).

<https://doi.org/10.1016/j.aquaculture.2023.739935>

Received 16 December 2022; Received in revised form 24 June 2023; Accepted 26 July 2023

Available online 3 August 2023

0044-8486/© 2023 The Authors. Published by Elsevier B.V. This is an open access article under the CC BY license (<http://creativecommons.org/licenses/by/4.0/>).

as 0.9 on dry weight (DW) basis; Papandroulakis et al., 2004); iii) a late reproductive maturation, with females first maturation at 77.9 cm total length (TL) (10.4 years) and all being mature at 90 cm TL (15.2 years), and males first maturation occurring at 74.9 cm (9 years) and all being mature at 80 cm TL (10.9 years; Peres and Klippel, 2003); iv) a large ovarian fecundity, from 3 to 11.9 million eggs ($135\text{--}311$ oocytes \times g^{-1} ; Peres and Klippel, 2003); iv) successful spontaneous reproduction of wild fish in captivity (Papadaki et al., 2018); v) great resistance to handling and adaptability to captivity, accepting commercial feed easily (Pérez et al., 2019); and vi) high market price and limited landings from wild fisheries, the last being reduced by 80–90% in the last decade (Pérez et al., 2019).

Research efforts conducted for developing wreckfish farming during the last decade, mainly through DIVERSIFY EU project, increased our knowledge on its biochemical composition and reproductive biology. Protein and lipid contents in muscle, liver and gonad, as well as viscerosomatic and gonado-somatic indexes from wild wreckfish were recently described (Linares et al., 2021). The natural spawning season, from autumn to winter, as well as the blood plasma profiles of the sex hormones during gametogenesis were also determined (Papandroulakis et al., 2004; Wakefield et al., 2013; Papadaki et al., 2018; Pérez et al., 2019). Although arrested oogenesis, failed oocyte maturation and non-fertilized spawned eggs were reproductive dysfunctions reported in wreckfish broodstocks, reproduction in captivity is possible without requiring hormonal induction (Papadaki et al., 2018; Pérez et al., 2019). In this sense, reproductive performance of wild specimens maintained in captivity differed depending the gender. Males were found in spermiation condition and producing good-quality sperm throughout the year, while only some females completed oogenesis, underwent oocyte maturation, and spawned spontaneously with a frequency of 4–5 days (Papandroulakis et al., 2008).

Variable spawning has been reported, and collected eggs often exhibit low fertilization, hatching and survival rates (Papadaki et al., 2018; Pérez et al., 2019). Furthermore, malformed individuals were observed in the rearing trials (Pérez et al., 2019). These malformations were initially identified as the swollen yolk sac syndrome due to inadequate nutrition of the broodstock (Gunasekera et al., 1998); and/or the blue sac disease, associated to early exposure to toxic compounds (Brzuzan et al., 2007). Up to now, wreckfish larvae were successfully reared very rarely (Pérez et al., 2019). Indeed, problems in larval culture have been recognized as the major difficulty in the development of mass juvenile production of different grouper species such as the hapuku wreckfish (*Polyprion oxygeneios*; Linares et al., 2021).

The high larval mortality rate in marine fish larvae is commonly associated to poor egg quality and/or suboptimal conditions during embryonic and larval development, leading to a high incidence of severe skeletal deformities (Seoka et al., 2003; Boglione et al., 2013a). Among the different abiotic conditions reported to affect fish development, light spectra and intensity as well as photoperiod, are known to be critical for larval development and survival (Boglione et al., 2013a). Since most fishes are visual feeders, specific light intensity is required to warrant proper live prey and microdiets capture to sustain normal larval development, among other physiological and biochemical processes (reviewed in Ruchin, 2021). While total darkness results in 100% mortality, too much light intensity can be stressful or even lethal (reviewed in Boeuf and Le Bail (1999)). Furthermore, light spectra and intensity also affect initial swim bladder inflation. Both lack of swim bladder inflation and its overinflation was shown to evolve into vertebrae anomalies (reviewed in Boglione et al., 2013a). Also, as fish are poikilotherm species, water temperature has significant effects on growth, differentiation and survival rates (Boglione et al., 2013a). Suboptimal water temperature during the embryonic and yolk-sac larval stages lead to early defects such as abnormalities of the primordial marginal fin fold, jaws, notochord and pericardial oedema (Polo et al., 1991). Indeed, high temperatures during early stages may induce craniofacial and morphological alterations in fish, most probably due an advanced skeletal

development (Cordova-de la Cruz et al., 2022). Increased incidence of anomalies affecting the vertebral column were reported in some fish species when eggs were incubated under higher temperatures (Wargelius et al., 2005; Dionísio et al., 2012). Therefore, to optimize light intensity and water temperature to be applied during fish early stages in new species, understanding how fish skeleton develops normally, detecting the types and incidences of skeletal deformities is recognized as a basic step for improving larval survival and the quality of the produced juveniles (Fernández and Gisbert, 2011; Boglione et al., 2013a; Koumoundouros et al., 2017). In fact, skeletal anomalies are mainly developed during larval stages, and severe deformities such as jaw, opercular and vertebral column deformities, have been shown to strongly decrease the growth potential and survival of fish (reviewed in Boglione et al., 2013a). Furthermore, since skeletal deformities affect body shape, their presence in fish of market size degrade the image of farmed fish, reducing its market price and the consumers' perception of farmed fish as a high quality product (Koumoundouros et al., 2017).

Here, an analysis of the fertilization, hatching, swim bladder inflation and survival rate of the wreckfish from 20 spawning events has been performed, describing for the first time the developmental sequences of the skeletal system as well as the main skeletal deformities in captive-reared wreckfish. Also, the influence on larval survival and the incidence of skeletal deformities of the temperature and the light intensity at water surface during endotrophic and exotrophic wreckfish larval stages has been explored. The present research work represents an important step forward towards the proper identification of larval-rearing bottlenecks, and outlining future research efforts to develop a successful, efficient and high-quality wreckfish farming.

2. Materials and methods

2.1. Ethical statement

Fish facilities from the Centro Oceanográfico de Vigo are officially registered at the competent National authorities (REGA ES360570189801) and had the pertinent permits for conducting fish experiments. Larval rearing trials and sampling procedures were previously approved by the Committee of Research Ethics of the University of Oviedo (Approval number ES360570189801/15/FUN.01/FIS.02). All experiments were performed following the ARRIVE guidelines (Percie Du Sert et al., 2020), and according to 2010/63/EU of the European Parliament and Council, guideline 86/609/EU of the European Union Council and Spanish legislation (Royal Decree 53/2013) for animal experimentation and welfare.

2.2. Breeder maintenance

Two wreckfish broodstocks (with 5 and 4 animals) were created and maintained at the Centro Oceanográfico de Vigo. Broodstock S1 includes 1 male (11.7 kg of wet body weight (BW) and 87.5 cm of TL) and 2 female (with average 20.92 ± 6.18 kg BW and 94 ± 2.82 cm TL) and one specimen with undetermined sex (6.15 kg BW and 70 cm TL). Broodstock S2 contains 1 male (14.2 kg BW and 91 cm TL) and 3 female (with average 19.76 ± 2.82 kg BW and 101.33 ± 6.5 cm TL). S1 and S2 broodstock were hosted in large tanks (110,000-L). Water temperature and photoperiod varied along the year according to the geographic region of Northwest Spain (Vigo, $42^{\circ}14'09''N$ and $8^{\circ}43'36''W$). Average water temperature was 15.4 ± 2.0 °C, with a salinity of 35 ppt, and 7.0 ± 0.6 mg L^{-1} of dissolved oxygen. Fish were fed with onsite prepared moist pellets containing 34.8% of fish meal (Fish Breed - M, Inve, Thailand), 14.8% of mackerel (*Scomber scombrus*), 14.8% of hake (*Merluccius merluccius*), 18% of mussel and 17.6% of squid. Fish were feed two times per week (Monday and Thursday) with a 1.14% of the total biomass.

2.3. Egg incubation

Wreckfish eggs were collected from the outflow and transferred into a 5–10 L jars. The total volume (mL) of the spontaneously spawned eggs, as well as the volume of the floating and non-floating eggs, were registered every morning of spawning days (Pérez et al., 2019). Then floating eggs were transferred to 140-L incubation tanks with a flow-through (1 µm filtered seawater) system (20% of water renewal per hour). General water conditions were as follows: 15.52 ± 1.0 °C, 35 ppt salinity, and 8.4 ± 0.1 mg L⁻¹ of dissolved oxygen. Dead (non-floating) eggs during incubation under natural photoperiod were daily removed and counted. Approximately, at 5 days after fertilization, hatched larvae were counted and transferred to larval rearing tanks. While a massive production of wreckfish larvae under a standard larval rearing protocol in medium-large volume tanks was conducted to describe the osteological development in this fish species (see below), the effect of water temperature and light intensity on larval performance (survival and quality) was tested in small volume tanks.

2.4. Standard larval rearing protocol

From each spawning event, hatched larvae were distributed in 500 or 1000-L cylindrical tanks at different densities (average initial density 48.71 ± 34.91 larvae L⁻¹, depending on the total number of hatched larvae obtained) and reared in a flow-through system with 1 µm filtered seawater and with the following conditions: 16.9 ± 0.21 °C, 35 ppt salinity and > 7 mg L⁻¹ of dissolved oxygen. Larvae were maintained under a natural photoperiod from 0 to 3 dph, 12 L: 12 D photoperiod and 900 lx of light intensity at water surface from 4 to 40 days post hatching (dph), and under natural photoperiod again afterwards. *IsochrYSIS galbana* and *Tetrasetelmis chuii* (5000–15,000 cells mL⁻¹ of *I. galbana* and 800–1600 cells mL⁻¹ of *T. chuii*) were added to the water from 8 to 24 dph as green water technique. During this period, larvae were reared combining a static system from 09:00 to 17:30 h, and with a flow-through system from 17:30 to 09:00 h to achieve a 300% renewal of the tank volume.

Larval feeding sequence was as follows: rotifers enriched with Multigain were supplied from 6 to 21 dph in increasing amounts (from 3 to 10 rotifer per mL). *Artemia* nauplii was supplied from 12 to 33 dph in increasing amounts (from 0.5 to 3 nauplii per mL); and *Artemia* metanauplii enriched with Multigain was provided from 30 to 50 dph in increased amounts (from 0.5 to 2 metanauplii per mL). Live preys were provided 3 times (09:00, 14:00 and 16:00 h) per day. Cofeeding with *Artemia* and microdiet (G 0.2, Skretting, Norway) was performed from 30 to 50 dph, and larvae were exclusively fed on microdiets (G 0.2–0.5, Skretting, Norway) until 71 dph.

2.5. Sampling, hatching and survival

Fertilization, hatching, swim bladder inflation and final survival (until 71 dph) rates were evaluated. For skeletal analysis larvae were sampled at 3, 5, 6, 7, 8, 10, 11, 12, 13, 14, 15, 18, 19, 21, 22, 63, 65, 67, and 71 dph based on larval survival and development. A total number of 632 specimens were sampled, euthanized with phenoxyethanol (Sigma-Aldrich, Germany) overdose and fixed in buffered paraformaldehyde (pH 7.4) during 24 h at room temperature for the analysis of osteological development. Standard length (SL; or notochord length in preflexion and flexion larvae) was recorded individually after post-staining. Since fixation and staining procedures are known to shrink larvae, values provided for SL might represent infraestimations of the real fish length, and therefore considered as reference values with caution when working with *in vivo* samples.

2.6. Effect of water temperature during endotrophic stage

Recently fertilized eggs (1–3 h post fertilization) from a single

spawning event were distributed in 5 L floating net pens and incubated until 7 dph at two different temperatures: 13.5 ± 0.5 or 16.0 ± 0.3 °C. Spawned eggs were obtained at 13.5 °C and temperature was increased at 1 °C per day in the experimental group incubated at 16 °C. Each thermal treatment was conducted in triplicate with up to 100 larvae each cage. Up to 15 larvae per replicate (45 per experimental group) were collected at 3, 4, 5, 6 and 7 dph, euthanized and fixed. The incidence of skeletal deformities along development was compared in larvae reared at the two experimental incubation temperatures.

2.7. Effect of light intensity during larval rearing

Following the previously described larval rearing protocol, 6000 hatched larvae (3 dph) were distributed into 6 cylindrical tanks (100-L volume each). Larvae were reared under three different light intensities (600, 900 and 1200 lx) at water surface in duplicates. Survival rate at 21 dph was calculated, and the remaining larvae were collected, euthanized and fixed as previously described for the analysis of osteological development.

2.8. Skeletal examination

Fixed larvae were rinsed in distilled water and gradually dehydrated in increasing series of ethanol (EtOH) solutions (25, 50, 75, and 100%). An acid-free double-staining protocol was performed as in Fernández et al. (2018), but adapted to wreckfish larvae. Briefly, EtOH solution was removed and larvae were immersed in a cartilage staining solution (0.02% Alcian blue 60 mM MgCl₂; Sigma-Aldrich, Madrid, Spain) for 6 h, washed with distilled water, and immersed in a bone-staining solution (0.005% alizarin red S; Sigma-Aldrich, Madrid, Spain) for 1 h. Larvae were washed in distilled water and bleached in a 1.5% hydrogen peroxide and 1% hydroxide potassium solution for up to 45 min. Every 5 to 10 min, the clearance of specimens was checked. Afterward, specimens were maintained (up to few days) within a 1% hydroxide potassium solution until the 80% of the natural pigmentation was removed. Finally, specimens were gradually (using 20, 50, and 75% glycerol solution series) transferred to a 100% glycerol solution, where they were stored until skeletal analysis was performed.

To evaluate the skeletal ontogeny as well as the type and the incidence of skeletal deformities found in stained fish, the following procedures were applied. First, fish with severe skeletal deformities (potentially affecting fish growth) were excluded from the analysis of the ontogenetic development of the skeletal system. In order to identify and quantify the degree of mineralization of the skeleton and the incidence of skeletal deformities, specimens were placed under a Leica MZ8 (Germany) stereomicroscope. The skeletal elements that appeared at each specimen were identified and counted (e.g. number of vertebral bodies, hypurals, etc.), while its degree of mineralization was evaluated as in cartilaginous stage, at the onset of ossification and/or at advanced ossification (when almost all the structure was ossified). The nomenclature used for the different skeletal elements was according to Faustino and Power (1998, 1999, 2001) and Bird and Mabee (2003). To evaluate the incidence of jaw and opercular deformities along the development, specimens were separated into 4 different size classes: < 4 mm SL ($n = 17$), 4–5 mm SL ($n = 251$), 5–6 mm SL ($n = 245$), and > 6 mm SL ($n = 119$). Incidence of vertebral and caudal fin deformities were only assessed in specimens that had a fully ossified skeleton ($n = 8$).

2.9. Statistical analysis

Data is presented as mean \pm standard deviation (SD) and was checked for normality (Kolmogorov–Smirnov test) and homoscedasticity of variance (Bartlett's test). Significant differences were detected by one-way ANOVA and Student's *t*-test. The Tukey multiple-comparison test was used to detect differences among experimental groups when identified by a one-way ANOVA. Significance was set at $P < 0.05$.

Statistical analysis was done using GraphPad 8.0 Software (San Diego, CA, USA).

3. Results

3.1. Egg fertilization, hatching, swim bladder inflation and survival rates

In this study, 20 spawning events were recorded during the spawning season of 2022. The average rates of fertilization, hatching, swim bladder inflation and survival (until 71 dph) are presented in Table 1. Swim bladder inflation has been first seen at 7 dph, with around 60% of the fish showing inflated swim bladder at 11 and 25 dph.

3.2. Ontogenetic development of the skeleton in wreckfish

Wreckfish larvae showed a linear growth in terms of standard length (SL; $y = 0.0942x + 3.8218$; with $R^2 = 0.7247$) from 3 to 71 dph (Supplementary Fig. 1). The frequency distribution by size class of wreckfish (*Polyprion americanus*) larvae sampled for skeletal development examination is included in Supplementary fig. 2. The first cartilage structures to appear were those located in the cranium (Fig. 1). The ethmoid plate, auditory capsule, ceratobranchials 1–2, Meckel's cartilage, quadrate, hyosymplectic cartilage and sclerotic elements were the first visible as cartilage structures in wreckfish larvae with 4 mm of SL. The taenia marginalis posterior, parasphenoid, parietal, supraoccipital, pterotic, prootic, opercle, basioccipital, ceratobranchials 1–5, maxilla, premaxilla, quadrate, hyosymplectic cartilage, dentary, and angular were slightly mineralized structures in larvae ranging 4–5 mm of SL. At 5–6 mm of SL, larvae showed almost all the skeletal structures composing the cranial region as fully mineralized structures. In general, most cranial structures underwent chondral ossification and most of them were completely ossified in larvae of 7–9.5 mm of SL, with the exception of the infraorbitals 2–4, which appeared to be only fully ossified in larvae ranging 10.5–14 mm of SL.

The appendicular skeleton of pectoral and pelvic fins also starts to be developed in larvae ranging 4–6 mm of SL (Fig. 2). In this case, cleithrum was the unique structure undergoing intramembranous ossification, being already formed in larvae with <4 mm of SL. The cartilaginous structures present at this size were the fin plate, coracoid anterior process and coracoid posterior process. The post-cleithrum and supra-cleithrum appeared as slightly mineralized structures in wreckfish larvae with 5–6 mm of SL. The last skeletal structures appeared in the pectoral fins were the coracoid, actinost, scapula, and soft rays in larvae ranging 6.5–14 mm of SL. In larvae with the same size the basipterygium and metapterygium were also observed as fully mineralized structures in the pelvic fins, while soft rays and spines started to be gradually developed in larvae at this size range. Dorsal and anal fins start to be formed from 5 mm of SL onwards, first with dorsal and ventral rays and dorsal and ventral pterygiophores afterwards.

In average, axial skeleton (Fig. 3) of wreckfish larvae was composed by 26 ± 0.53 vertebra, including 2 cephalic, 10 pre-haemal, 12 haemal and 2 pre-ural vertebra. In larvae with 4.25 mm SL, neural process (Np)

Table 1

Fertilization, hatching, swim bladder inflation and survival rates of wreckfish under breeders' and standard larval rearing protocol.

	Mean \pm SD	n
Fertilization rate (%)	61.75 \pm 34.62	20
Hatching rate (%)	4.52 \pm 9.27	20
Swim bladder inflation (%)		
at 11 dph	61.11 \pm 3.72	2
at 25 dph *	63.33	1
Survival rate at 71 dph (%)	0.01 \pm 0.00	2

Dph, days post hatching; n, number of spawning events or larval batches analyzed; * Due to the low survival and the sampling effort at previous developmental stages, only a single larval batch has been sampled at this age (no SD value is available).

from cephalic and pre-haemal vertebra 1–4, as well as parapophyses and haemal process (Pp 1–5, Hp 1–12) were already visible as cartilaginous structures before their respective vertebra, and being slightly mineralized in larvae with 5 mm of SL. Regarding vertebral bodies, mineralization proceeds dorsal to ventral in cephalic and pre-haemal vertebra, and in both directions in haemal vertebra. The first vertebra to show mineralization of the chordacentra were 1–8th vertebra, but occurring at a slow rate. In contrast, although chordacentra mineralization of 9–24th vertebra started later on, it proceeds faster and the mineralization of the chordacentra ring was completed earlier than in 1–8th vertebra. A slight mineralization started to be patent in the case of cephalic and the first pre-haemal vertebra in larvae ranging 4–5 mm of SL, while the mineralization in vertebra 4–6 was observed in larvae ranging 5–6 mm of SL. The rest of vertebral bodies (7–24) showed mineralization in larvae ranging 6–7 mm of SL, being all structures of the axial skeleton fully mineralized in larvae with 7 mm of SL, including the ribs.

The development of the caudal fin complex (Fig. 4) started with the appearance of the hypural 1 and the modified haemal process from pre-ural vertebra 3 (PU3) and 2 (PU2) in larvae with 4.25 mm of SL, as cartilage elements. In larvae of 5 mm of SL some other cartilaginous structures including modified Ns from PU3 and neural arch (Na) from PU2 were observed, followed by hypurals 2–5, parahypural and epural 2 as cartilage elements, and the bone mineralization of the pre-ural vertebra 2 and 3. Most of the elements, including dorsal and ventral rays, started to be slightly mineralized in larvae with 6–6.5 mm of SL, and being fully ossified in larvae with 7 mm of SL.

3.3. Incidence of skeletal deformities

Among the 632 individuals analyzed during larval development, 55.8% showed at least one skeletal deformity. In the cranial region, first identified skeletal deformities in larvae with <4 mm of SL were short upper jaw (10%) and curved lower jaw (23%) (Fig. 5a). In larvae ranging 4–5 mm of SL, the most common deformity was curved lower jaw (63%), followed by right (37%) and left operculum (28%) deformities (Fig. 5b). The incidence of these deformities decreased to 47% (curved lower jaw), 25% (left operculum) and 24% (right operculum) in larvae ranging 5–6 mm of SL (Fig. 5c). In larvae with >6 mm of SL the most affected structure was lower jaw (34%), with 21% of the larvae showing shorter lower jaw, 8% longer lower jaw and 5% curved lower jaw. Also, 26% of larvae had shorter upper jaw, 9% left operculum deformity and 6% right operculum deformity (Fig. 5d).

Along the vertebral column, deformities were mainly found at 9–18th vertebra, with a variable degree of incidence (Fig. 6a). The most common deformity was vertebral compression, displacement and fusion. Haemal vertebra 1, 2 and 3 were the most abundantly deformed (44.4% of the larvae). Most of these deformities were associated to lordosis, found in the 50% of the larvae, although none of the analyzed larvae showed kyphosis or scoliosis (Fig. 6b).

Finally, at the caudal fin complex (Fig. 7), all elements showed deformities except hypural 1. The highest incidence of deformity was found at the neural arch (62.5%), while the lowest was reported at the hypurals 3–4 and epurals 1–2 (12.5%).

3.4. The effect of temperature during early development

The incidence of deformities in wreckfish embryos exposed to different temperatures (13.5 ± 0.5 and 16.0 ± 0.3 °C) from fertilization to 7 dph is shown in Fig. 8. Among the 496 individuals analyzed, 53.42% showed curved lower jaw deformity. Results along development showed a similar decrease on the incidence of curved lower jaw when wreckfish embryos were exposed to both temperatures, without significant differences between both experimental groups at each sampling point ($P > 0.05$). Nevertheless, the decrease was significantly different in embryos exposed to 16 °C when compared 3 and 7 dph larvae ($P < 0.05$).

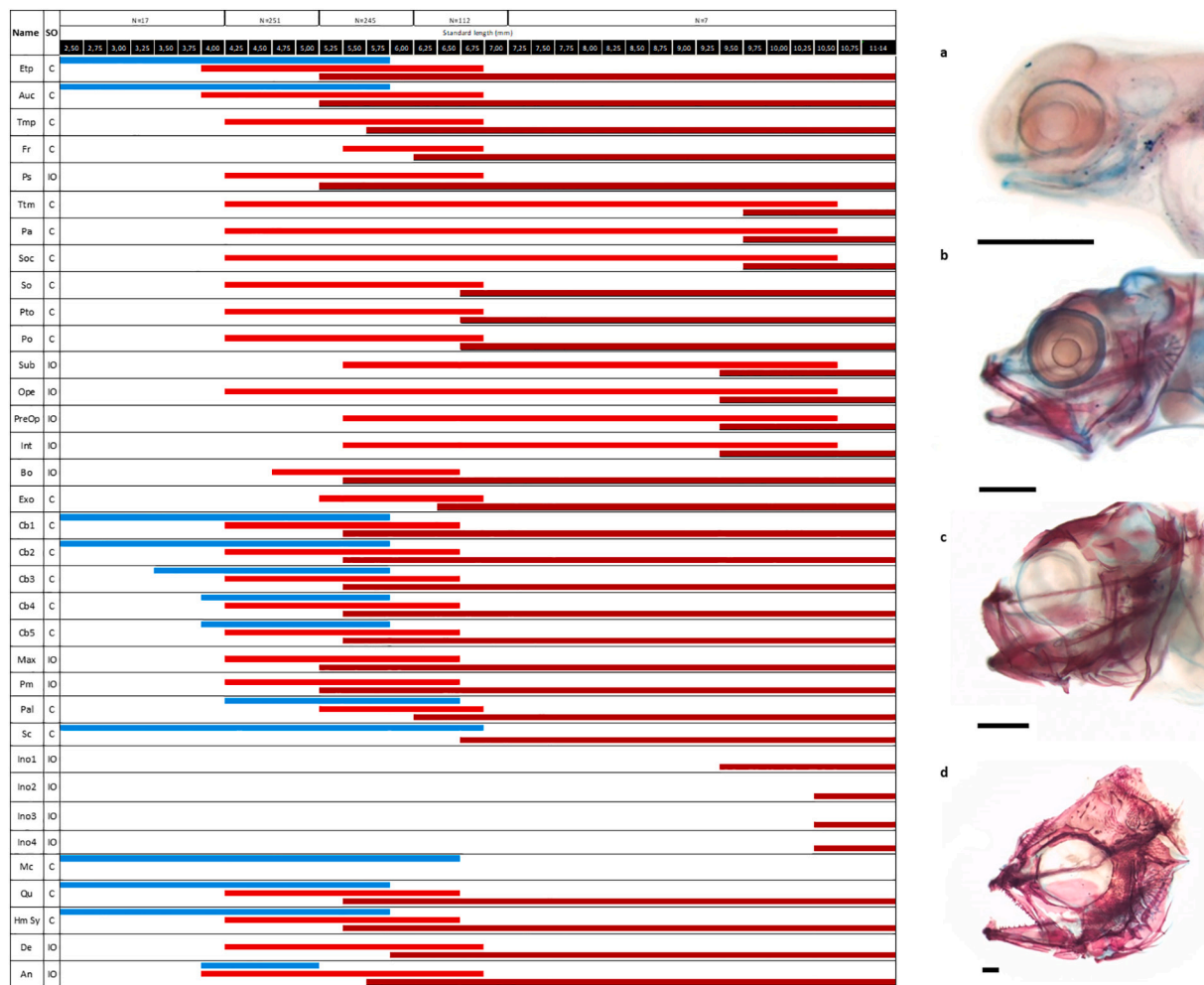


Fig. 1. Schematic representation of the skeletal formation of the main structures from the cranium of wreckfish (*Polyprion americanus*) during larval development, according to their standard length (SL). While the number of the larvae analyzed and their SL are shown at the top, on the right side some representative images of the cranium in wreckfish larvae are included. Head of a larvae with 5 days post hatch (dph) and 4.91 mm of SL (a), 14 dph and 5.01 mm of SL (b), 21 dph and 6.1 mm of SL (c), and 65 dph and 11.71 mm of SL (d). Scale bar = 500 μ m. Color lines: *blue*, the structure is in cartilage stage; *light red*, the structure is slightly mineralized; *dark red*, the structure is fully mineralized. The process of skeletal ossification (SO) is represented as C, chondral ossification; and IO, intramembranous ossification. Skeletal structures: An, angular; Auc, auditory capsule; Bo, basioccipital; Cb1–5, ceratobranchials 1–5; De, dentary; Etp, ethmoid plate; Exo, exoccipital; Fr, frontal; Hm Sy, hyosymplectic; Ino1–4, infraorbitals 1–4; Int, interopercula; Max, maxilla; Mc, Meckel’s cartilage; Ope, opercula; Pa, parietal; Pal, palatine; Pm, premaxilla; Po, prootic; PreOp, preopercula; Pto, pterotic; Ps, parasphenoid; Qu, quadrate; Sc, sclerotic; Soc, supraoccipital; Sub, subopercula; Tma, taenia marginalis anterior; Tmp, taenia marginalis posterior; Ttm, taenia tecti medialis. (For interpretation of the references to color in this figure legend, the reader is referred to the web version of this article.)

3.5. The effect of light intensity during larval rearing

Although mean survival rate of larvae reared at 600 lx ($0.15 \pm 0.2\%$) tended to be lower than those reared at 900 or 1200 lx (0.6 ± 0.3 and $0.7 \pm 0.3\%$), no significant differences were reported (ANOVA, $P > 0.05$). No significant differences were also reported in terms of growth in length, with values ranging from 5.3 ± 0.3 to 5.9 ± 0.1 mm of SL, nor in the incidence of skeletal deformities (ANOVA, $P > 0.05$). Incidence of deformities at head structures in wreckfish of 21 dph were represented as mean of the 2 biological replicates, with the exception of larvae from 600 lx, where only larvae from one replicate survived (Fig. 9). In larvae reared at 600, 900 and 1200 lx, curved left and right opercula were the most common deformities (from 30.56 ± 19.64 to $42.50 \pm 24.74\%$ and from 33.33 ± 0.0 to $44.44 \pm 15.71\%$, respectively), followed by curved lower jaw deformity. In this case, incidences ranged from 0.0 ± 0.0 to $25.00 \pm 11.78\%$, being not detected in larvae from 600 lx group but with the highest identified frequency in larvae from 1200 lx group.

4. Discussion

Considering that wreckfish is declared as Near Threatened (Collette et al., 2015) and the seventh most suitable species for aquaculture diversification out of 27 candidate species (Quémener et al., 2002), there is an urgent need and interest in advancing on its farming technology and husbandry practices (Pérez et al., 2019). This would warrant the availability of this highly appreciated product on the market at an affordable price without hampering the conservation of the natural stocks. On the contrary, the rearing of this (and other) species under controlled conditions (fish farms) will also contribute to restocking activities and recover the natural stocks in a nearest future (Huntingford, 2004; Taylor et al., 2017).

After achieving successful maintenance and reproduction of wild breeders in captivity (Papadaki et al., 2018), last efforts have been focused on defining an initial standard larval rearing protocol (Pérez et al., 2019). Here, although the low larval survival limited the number of analyzed specimens with higher SL than 7 mm, and the corresponding osteological descriptions, a basic knowledge on how the skeletal system

Name	SO	N=17					N=251					N=245					N=112					N=7				
		Standard length (m.m)																								
		2.50	2.75	3.00	3.25	3.50	3.75	4.00	4.25	4.50	4.75	5.00	5.25	5.50	5.75	6.00	6.25	6.50	6.75	7.00	7.25	7.50	7.75-14			
Cl	IO	[Red bar from 3.75 to 6.75]															[Red bar from 5.25 to 7.75-14]									
Fp	C	[Blue bar from 2.50 to 6.75]																								
Co Ap	C	[Blue bar from 2.50 to 6.75]															[Red bar from 6.25 to 7.75-14]									
Co Pp	C	[Blue bar from 2.50 to 6.75]															[Red bar from 5.25 to 7.75-14]									
Post Cl	IO	[Red bar from 5.25 to 6.75]															[Red bar from 5.75 to 7.75-14]									
Sut	IO	[Red bar from 5.25 to 6.75]															[Red bar from 5.75 to 7.75-14]									
Co	C	[Red bar from 6.25 to 7.75-14]																								
Act	C	[Red bar from 6.25 to 7.75-14]																								
Sca	IO	[Red bar from 6.25 to 7.75-14]																								
Bp	IO	[Red bar from 6.25 to 7.75-14]																								
Me	IO	[Red bar from 6.25 to 7.75-14]																								
Dr	IO	[Light grey bar from 5.00 to 5.75]					[Dark grey bar from 5.25 to 6.00]					[Dark grey bar from 5.75 to 6.50]					[Dark grey bar from 6.25 to 7.75-14]									
Vr	IO	[Light grey bar from 5.00 to 5.75]					[Dark grey bar from 5.25 to 6.00]					[Dark grey bar from 5.75 to 6.50]					[Dark grey bar from 6.25 to 7.75-14]									
Dp	C	[Light grey bar from 5.00 to 5.75]					[Dark grey bar from 5.25 to 6.00]					[Dark grey bar from 5.75 to 6.50]					[Dark grey bar from 6.25 to 7.75-14]									
Vp	C	[Light grey bar from 5.00 to 5.75]					[Dark grey bar from 5.25 to 6.00]					[Dark grey bar from 5.75 to 6.50]					[Dark grey bar from 6.25 to 7.75-14]									
S	C	[Dark grey bar from 6.25 to 7.75-14]																								
R	C	[Dark grey bar from 6.25 to 7.75-14]																								

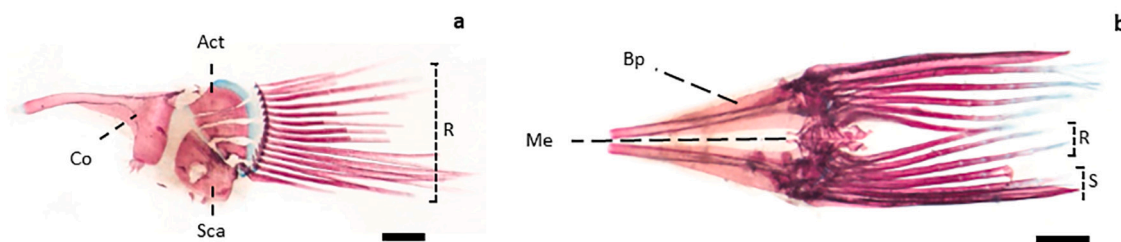


Fig. 2. Schematic representation of the skeletal formation of the main structures from the fins of wreckfish (*Polyprion americanus*) during larval development, according to their standard length (SL). While the number of the larvae analyzed and their SL are shown at the top, at the bottom some representative images of the elements composing the pectoral (a) and pelvic (b) fins in wreckfish larvae are included. Scale bar = 500 μ m. Color lines: *blue*, the structure is in cartilage stage; *light red*, the structure is slightly mineralized; *dark red*, the structure is fully mineralized; *light grey*, half of the elements are visible; *dark grey*, all elements composing these structures are formed; *black*, structures are fully mineralized. The process of skeletal ossification (SO) is represented as C, chondral ossification; and IO, intramembranous ossification. Skeletal structures: Act, Actinost; Bp, Basipterygium; Cl, cleithrum; Co Ap, coracoid anterior process; Co Pp, coracoid posterior process; Co, coracoid; Dp, dorsal pterygiophores; Dr, dorsal rays; Fp, cartilaginous fin plate; Me, metapterygium; S, spine; Sca, scapula; R, soft ray; Post Cl, postcleithrum; Sut, supracleithrum; Vp, ventral pterygiophores; Vr, ventral rays. (For interpretation of the references to color in this figure legend, the reader is referred to the web version of this article.)

of wreckfish is formed along larval development, and which are the most frequent skeletal deformities under this standard protocol is provided. Also, how abiotic factors - such as rearing temperature (during early development) and light intensity (during larval development) - affect skeletal development was also explored.

Acceptable fertilization rate of spawned eggs is basic to warrant a successful larval rearing. The rate here reported in wreckfish (61%) is comparable with the 68% observed for its sister species, the hāpuku wreckfish (*Polyprion oxygeneios*; Symonds et al., 2014). The low survival rate (< 0.1%) in wreckfish larvae is also in line with previous results from our research group and collaborators (Pérez et al., 2019; Linares et al., 2021). Inconsistent and low survival values (0.0 to 5.66%) were

also reported in hāpuku wreckfish (Symonds et al., 2014), despite of the higher progress on the farming of this fish species (including the availability of a F2 generation nowadays). Larval hatching and survival rates in wreckfish represent nowadays the major limitation for farming this species once the spontaneous reproduction of wild captured specimens has been overcome (Papadaki et al., 2018; Pérez et al., 2019). Limited hatching and low survival might be associated to genetic inbreeding, poor egg quality and/or suboptimal conditions during embryonic and larval development. Previous research on genetic diversity of the two maintained broodstocks do not support the hypothesis of low wreckfish hatching and survival due to genetic inbreeding (Matusse et al., 2016). The use of different egg incubation systems and conditions (here not

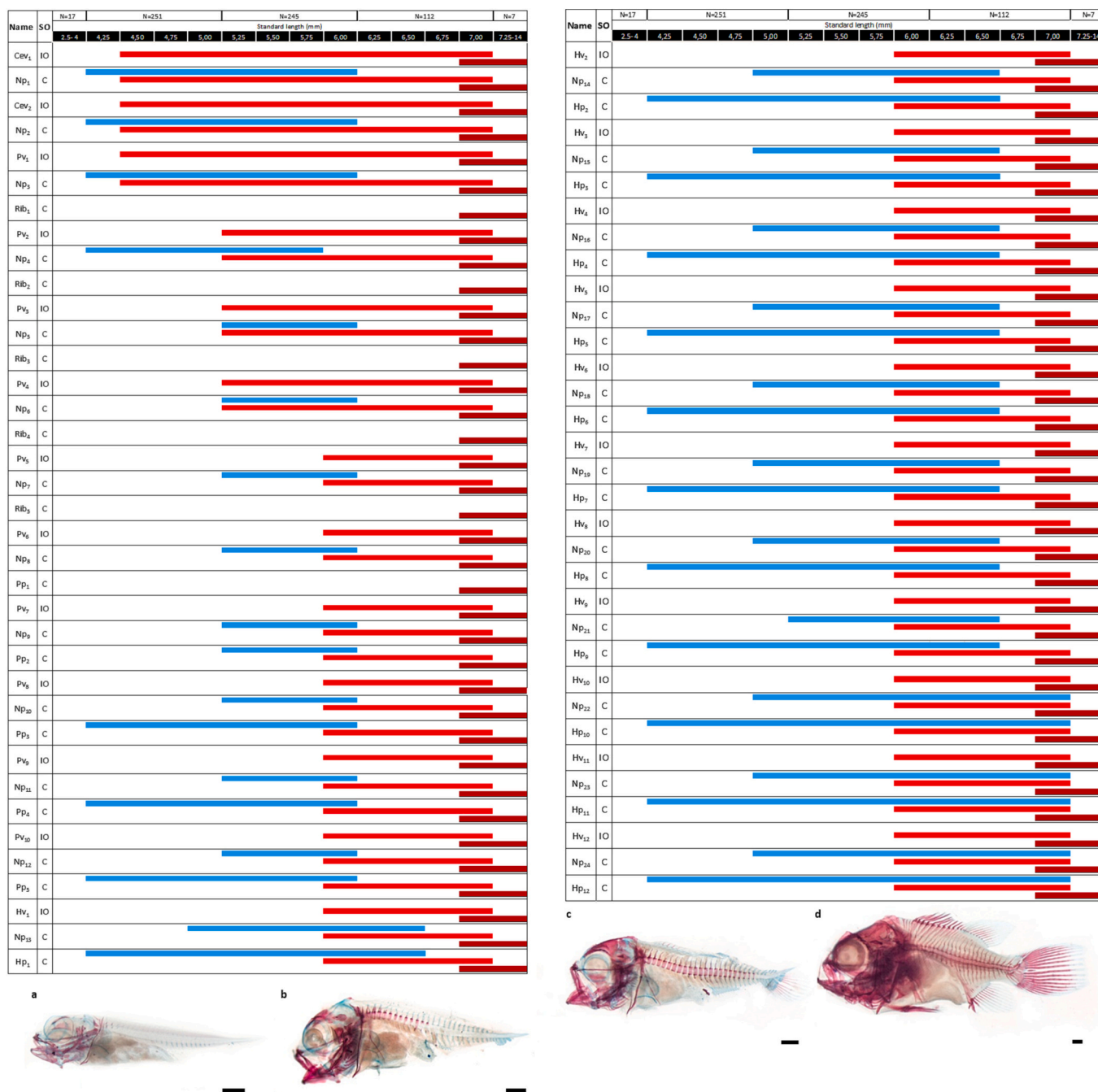


Fig. 3. Schematic representation of the formation of the axial skeleton of wreckfish (*Polyprion americanus*) during larval development, according to their standard length (SL). While the number of the larvae analyzed and their SL are shown at the top, at the bottom some representative images of larvae with a different degree of development of the vertebral column are included. Larvae with 14 days post hatch (dph) and 5.45 mm of SL (a), 21 dph and 5.41 mm of SL (b), 21 dph and 6.1 mm of SL (c), and 65 dph and 11.71 mm of SL (d). Scale bar = 500 μ m. Color lines: *blue*, the structure is in cartilage stage; *light red*, the structure is slightly mineralized; *dark red*, the structure is fully mineralized. The process of skeletal ossification (SO) is represented as C, chondral ossification; and IO, intramembranous ossification. Skeletal structures: Cev, cephalic vertebrae; Cv, caudal vertebrae; Hp, haemal process; Hv, haemal vertebra; Np, neural process; Pp, parapophysis; Pv, pre-haemal vertebra; Rib, ribs. (For interpretation of the references to color in this figure legend, the reader is referred to the web version of this article.)

described) support the hypothesis that breeders' nutrition is not fulfilling all the nutritional requirements of this fish species for successful embryonic development and proper hatching.

4.1. Development and incidences of skeletal deformities provides key knowledge for improving wreckfish larval rearing

Marine fish larval development involves dramatic changes in structure in a very short period, encompassing organogenesis and

metamorphosis (Fuiman et al., 1998; McMenamin and Parichy, 2013). The use of several predictors has been proposed to overcome major constraints in commercial production (reviewed in Koumoundouros et al., 2017). For instance, blastomere morphology, floating percentage, fertilization percentage, and egg and lipid vesicle diameter were considered for a relatively rapid and accurate assessment of the potential hatching and survival of fertilized eggs in different fish species, including hapuku wreckfish (Kohn and Symonds, 2012). Although this may increase the efficiency of hatchery work (prioritizing the use of

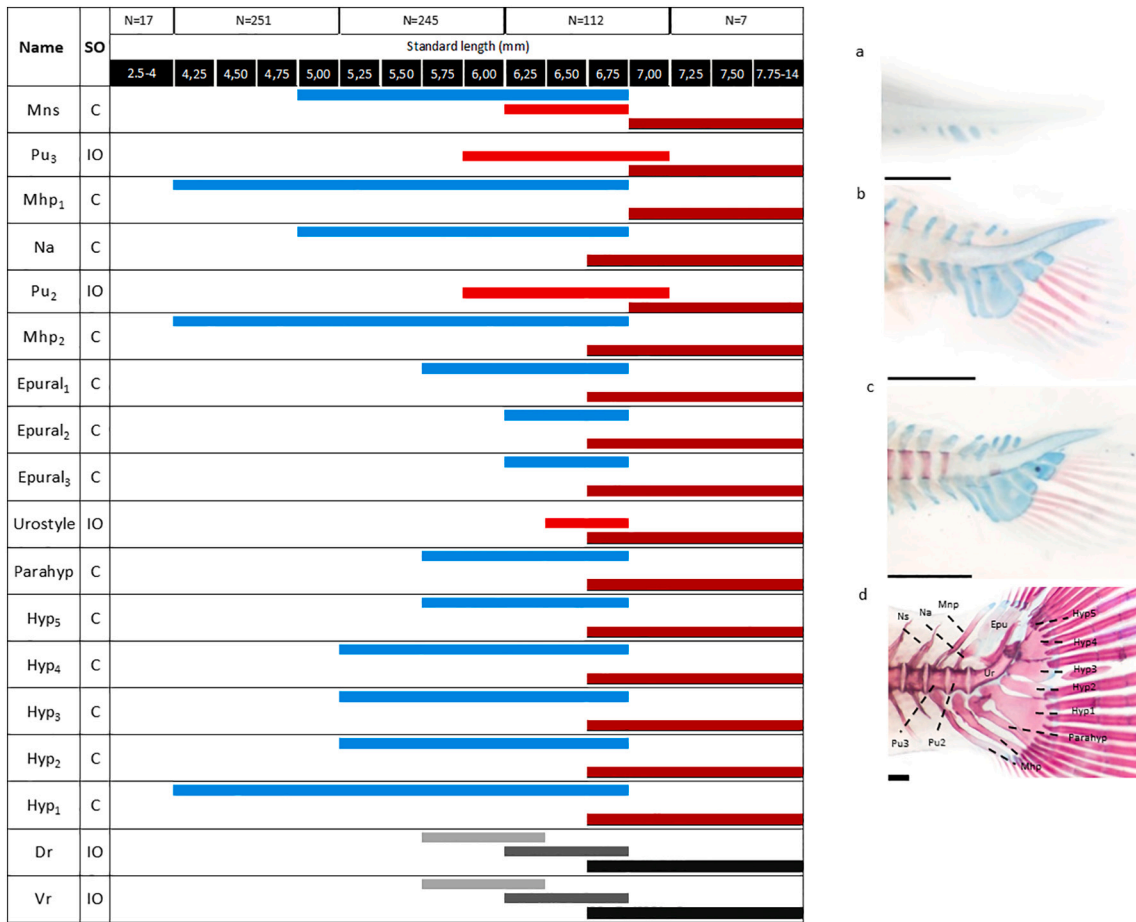


Fig. 4. Schematic representation of the skeletal formation of the caudal fin complex of wreckfish (*Polyprion americanus*) during larval development, according to their standard length (SL). While the number of the larvae analyzed and their SL are shown at the top, on the right side some representative images of caudal fin complex with a different degree of development are included. Larvae with 14 days post hatch (dph) and 5.01 mm of SL (a), 21 dph and 5.41 mm of SL (b), 21 dph and 6.1 mm of SL (c), and 65 dph and 11.71 mm of SL (d). Scale bar = 500 μm. Color lines: *blue*, the structure is in cartilage stage; *light red*, the structure is slightly mineralized; *dark red*, the structure is fully mineralized; *light grey*, first elements are visible; *dark grey*, half of the elements composing these structures are formed; *black*, structures are fully mineralized. The process of skeletal ossification (SO) is represented as C, chondral ossification; and IO, intramembranous ossification. Skeletal structures: Dr, dorsal rays; Hp, haemal process; Hyp 1–5, hypurals 1–5; Mhp, modified haemal process; Mnp, modified neural process; Na, neural arch of PU2; Np, neural process; Parahyp, parahypural; Pu, preural vertebrae; Vr, ventral rays. (For interpretation of the references to color in this figure legend, the reader is referred to the web version of this article.)

incubators for only good quality eggs), this will not identify the specific problems and/or to solve them.

Understanding how fish skeleton develops, detecting the types and incidences of skeletal deformities might be a key and complementary step for improving larval survival and the quality of the produced juveniles (Fernández and Gisbert, 2011; Boglione et al., 2013a, 2013b; Koumoundouros et al., 2017). Once it is known when a structure starts to be developed, the potential factors inducing its abnormal development can be identified and thus, solutions/improvements can be explored. Therefore, although the description of some organs and structures has been already made for *P. oxygeneios* (Anderson et al., 2012) and *P. americanus* (Pérez et al., 2019), the specific and detailed description of the skeletal development of wreckfish using an acid free double staining procedure is here presented for the first time.

4.1.1. Osteological development is consistent with the wreckfish fast body growth

In general, teleost larval development seems to follow a common programed plan regarding the ontogenic sequence of skeletogenesis. First skeletal elements to appear in wreckfish larvae are those related to feeding (Meckel’s cartilage, ethmoid, and hyomandibular) or respiratory purposes (ceratobranchials and cleithrum) (Cubbage and Mabee,

1996; Faustino and Power, 1998; Fernández et al., 2018; Fernández et al., 2021), all of them located in the cranial region. The ossification of these structures also proceeds quite fast, showing an advanced ossification at 4–5 mm of SL. Cranial skeletal development was consistent with the observation of some structures without using specific dyes (e.g., alcian blue and alizarin red) such as jaw formation, mouth opening and increased body height in *P. americanus* and *P. oxygeneios* during early larval development (6–9 dph; Anderson et al., 2012; Pérez et al., 2019). Regarding the axial skeleton, the pattern of vertebral column development differs among fish species. In some species, first ossifying vertebral centra are those from the caudal region (e.g., in Atlantic thread herring (*Opisthonema oglinum*)), while in other species this first vertebral centra to ossify is located at the pre-haemal and anterior haemal regions (e.g., in Atlantic halibut (*Hippoglossus hippoglossus*)), being in both cases the ossification extended in both anterior and posterior directions (Richards et al., 1974; Lewis and Lall, 2006). Wreckfish axial skeleton ossification starts at the cephalic region and progressed in an anterior to posterior direction. The onset of vertebral ossification occurred quite early, in larvae ranging 4–5 mm of SL and proceeds very rapid, being completely ossified in larvae ranging 6–7 mm of SL. Particular centra ossification patterns have been reported for several other fish species, mainly sparids such as *Dentex dentex*, *Pagellus erythrinus*, *Sparus aurata*, *Pagrus major*

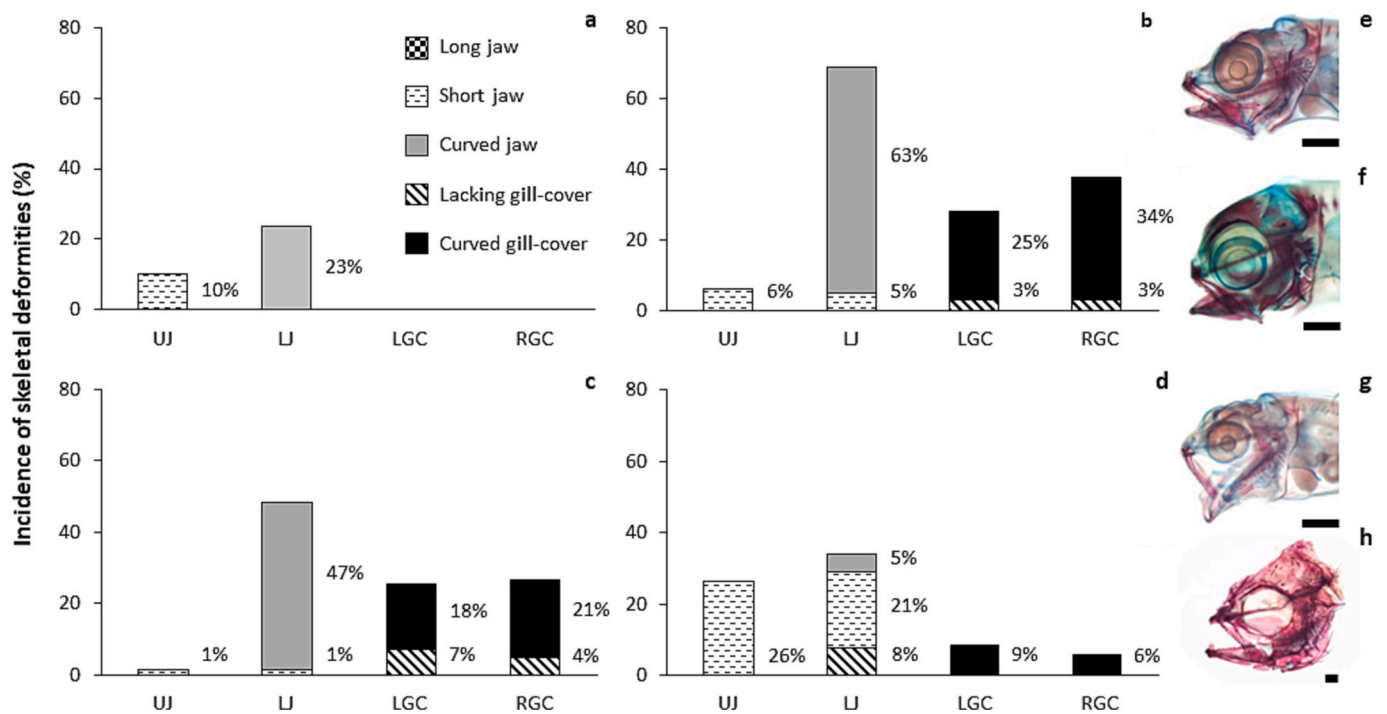


Fig. 5. Incidence (in %) of head deformities wreckfish (*Polyprion americanus*) during larval development according to 4 different size classes. Larvae with <4 mm of SL ($n = 17$) (a), larvae with 4–5 mm of SL ($n = 251$) (b), larvae with 5–6 mm of SL ($n = 245$) (c), larvae >6 mm of SL ($n = 119$) (d). Representative images of fish with normally developed jaws (e), short upper jaw (f), curved lower jaw (g), and longer lower jaw (h) are presented in the right side. Anatomical area: LJ, lower jaw; LGC, left gill-cover; RGC, right gill-cover; UJ, upper jaw. Scale bar = 500 μ m.

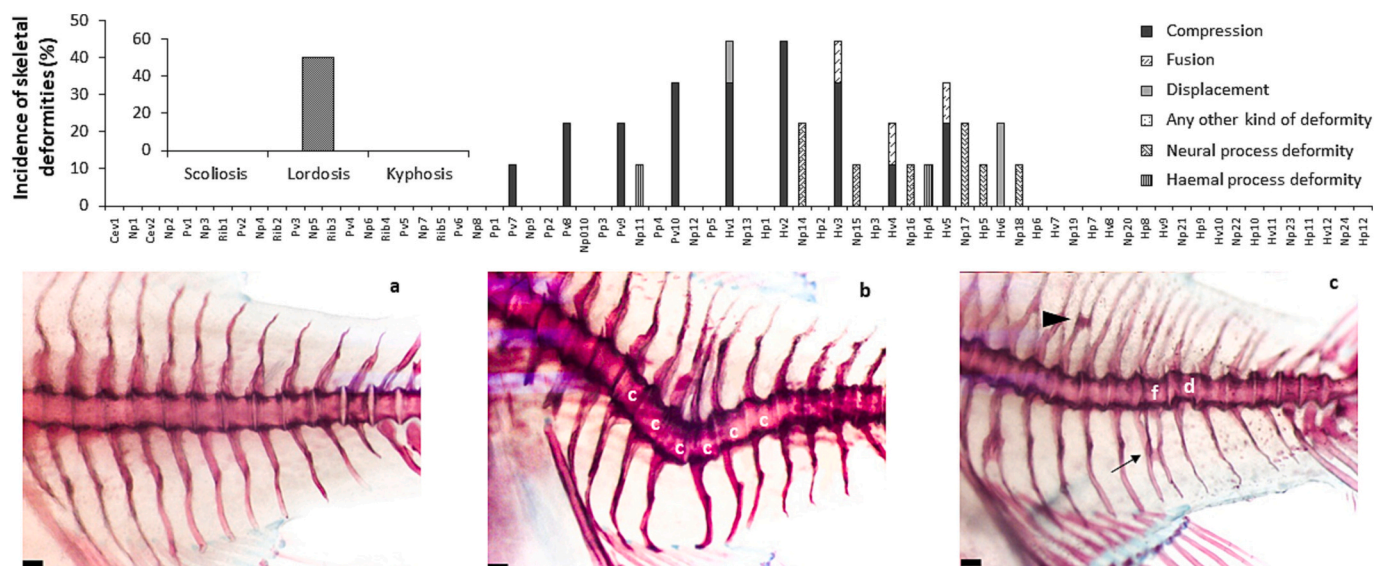


Fig. 6. Incidence (in %) and representative images of skeletal deformities along the axial skeleton in wreckfish (*Polyprion americanus*) larvae of 6.86–13.39 mm of SL ($n = 8$). Representative images of fish with normally developed axial skeleton (a), lordosis (b), and vertebral displacement and neural and haemal processes deformity (c). C, compression; D, displacement; F, fusion; Arrow head, neuro spine deformity; Arrow, haemal process deformity. Abbreviations in Fig. 3, Scale bar = 500 μ m.

(Matsuoka, 1982; Koumoundouros et al., 1997a; Faustino and Power, 1999; Sfakianakis et al., 2005) as well as cyprinids and pleuronectiforms (e.g., *Tinca tinca* and *Solea senegalensis*; Fernández et al., 2018, 2021). The vertebral development observed in wreckfish appears to follow the one commonly found in perciforms. Similarly, the development of the appendicular skeleton (paired and impaired fins) follows a common sequence in fish species, independently of the morphology and length of these fins and/or fish locomotion mode, with pectoral and caudal fins the first to be developed (Houde and Potthoff, 1976; Matsuoka, 1982;

Kusaka et al., 1994; Koumoundouros et al., 1997a; Faustino and Power, 1999; Fernández et al., 2018, 2021). The development of both skeletal systems (axial and appendicular) seemed to respond to the increased need for swimming activity and body position control for effective prey capture and predator escapee.

4.1.2. Incidence and typology of observed skeletal deformities identify potential causative factors and research needs

The high incidence of severe skeletal deformities is commonly

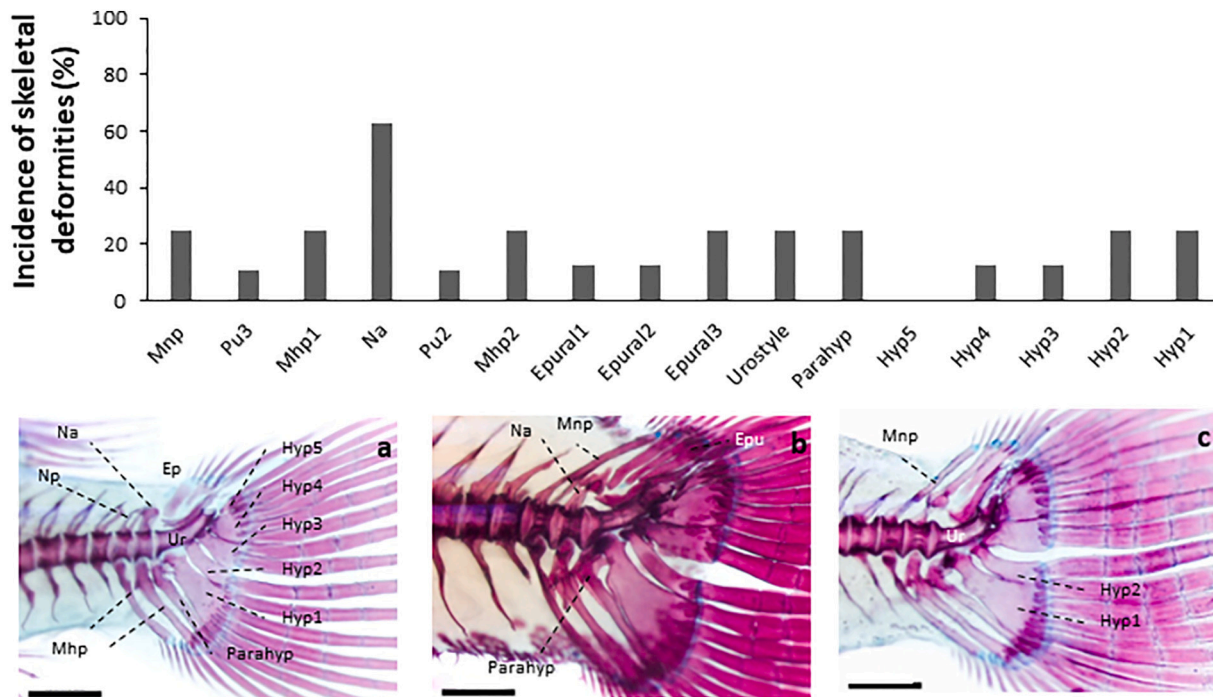


Fig. 7. Incidence (in %) and representative images of skeletal deformities of the caudal fin complex in wreckfish (*Polyprion americanus*) larvae of 6.86–13.39 mm of SL (n = 8). Representative images of fish with a caudal fin complex showing a deformity in the modified neural process (a), the neural arch and the modified haemal process of PU2 (b), and deformed modified neural process, neural arch, urostyle and fussed hypurals 1 and 2 (c). Abbreviations in Fig. 4 Scale bar = 500 μm.

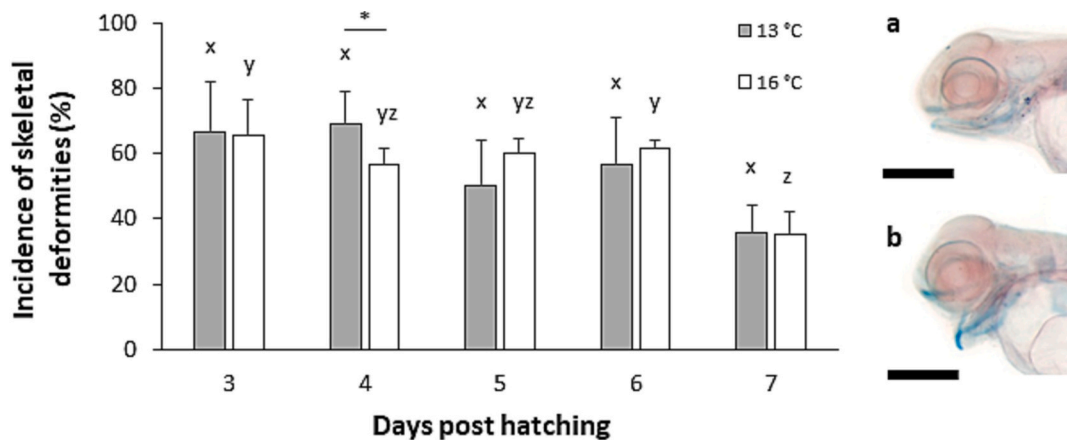


Fig. 8. Incidence (in %) and representative images of skeletal deformities of the lower jaw in wreckfish (*Polyprion americanus*) larvae when reared in different temperatures (13.5 ± 0.45 and 16.0 ± 0.3 °C). Representative images of larvae with normal jaw (a), and larvae with a curved lower jaw (b). Scale bar = 500 μm. Different letters at the top of the histograms within the same experimental group indicates a significant difference between sampling points (one-way ANOVA, $P < 0.05$; $n = 3$). Asterisk indicates significant differences between experimental groups at particular sampling points (Student *t*-test, $P < 0.05$; $n = 3$).

associated to a high larval mortality rate in marine fish larvae and to a poor image of farmed fish when deformed fish is sold at market size (Boglione et al., 2013a), reducing its market price and the consumers' perception of farmed fish as a high quality product (Koumoundouros et al., 2017). Although those affecting the body shape can be identified by direct visual inspection (Koumoundouros, 2010) such as previously performed in wreckfish (Pérez et al., 2019), double staining and X ray analyses might be helpful to identify not only less evident deformities that also hamper fish growth and survival (de Azevedo et al., 2017; Fernández et al., 2021), but also to hypothesize about the potential factors responsible for the appearance of such deformities. In the present study, among the 632 individuals analyzed along larval development, 55.75% showed at least one skeletal deformity. Among the severe deformities encountered in wreckfish larvae, jaw deformities were the first

to be detected and the most abundantly reported. Jaw deformities have been previously observed in other commonly farmed fish species (Barahona-Fernandes, 1982; Daoulas et al., 1991; Boglione et al., 2001; Cobcroft et al., 2001; Haga et al., 2002; Fernández et al., 2008, Fernández et al., 2021). Importantly, in wreckfish larvae from <4 to 4–5 mm of SL, an increasing rate (from 23 to 63%) was found for the most frequently reported jaw deformity type, the curved lower jaw. However, the incidence of this deformity progressively decreased (to 47 and 5%) afterward, in larvae with 5–6 and > 6 mm of SL. The pattern of incidences of this deformity along development seemed to be related with its severity, decreasing the viability of growing larvae as previously reported (Barahona-Fernandes, 1982). Most likely, fish with deformed jaws had an impaired ability to catch live prey (rotifers and *Artemia*; Haga et al., 2002) and would be one of the main reasons of low survival

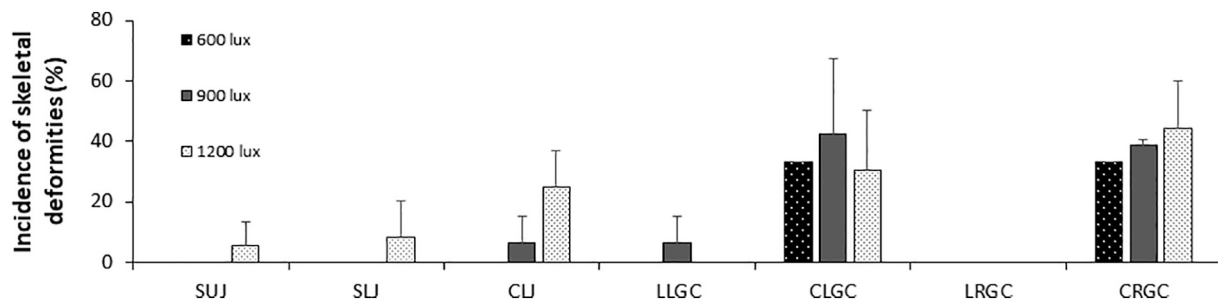


Fig. 9. Mean and standard deviation of the incidence (in %) of skeletal deformities in the head structures of wreckfish (*Polypriion americanus*) larvae reared under different light intensities (600, 900 and 1200 lx) at water surface. CLJ, curved lower jaw; CLGC, curved left gill-cover; CRGC, curved right gill-cover; LLGC, lacking left gill-cover; LRGC, lacking right gill-cover; SLJ, short lower jaw; SUJ, short upper jaw. Note that no error bars are shown in the histograms from 600 lx group, as only larvae from one replicate survived.

rate in wreckfish larval rearing. In previous reports, these jaw malformations were initially identified as swollen yolk sac syndrome and/or blue sac disease (Brzuzan et al., 2007). However, the lack of cardiac oedema in wreckfish larvae and the specific phenotype of curved lower jaw do not fit with that syndrome or disease. High vitamin A (retinoic acid, particularly) dietary content at first feeding has been shown to induce lower jaw deformities in flatfish species (*Paralichthys olivaceus*; Haga et al., 2002). Also, Atlantic salmon (*Salmo salar*) triploids were reported to be prone to show curved lower jaw, being linked to a vitamin and/or mineral (mainly phosphorus) deficiency, as well as environmental factors such as low dissolved oxygen, elevated temperature and husbandry practices (Sadler et al., 2001; Lijalad and Powell, 2009; Amoroso et al., 2016a; Fjellidal et al., 2016). Indeed, a higher incidence of curved lower jaw has been observed when Atlantic salmon was reared at high temperatures (14 versus 18 °C), and this was associated to an altered hormonal regulation of the cartilage development (Amoroso et al., 2016b). In our case, rearing temperature during early development seemed to not be the causative factor of such jaw deformity (comparing reared larvae at 13 and 16 °C; see below). Although other abiotic factors cannot be ruled out, present results suggested that low egg quality might be the most plausible cause of high incidence of lower jaw deformity and therefore, low hatching and survival rates.

Opercular deformities are the most frequent anomaly affecting cranial region in marine fish species such as *S. aurata*, and has attracted researchers' attention to identify and describe the timing of appearance, the aetiology and the different typologies observed (Koumoundouros et al., 1997b; Verhaegen et al., 2007; Ortiz-Delgado et al., 2014). Similar to jaw deformities, a decreasing pattern of opercular deformities in wreckfish larvae has also been found, although with a lower incidence: from 28 to 37% to 9–6% of left or right opercula deformities, respectively. This pattern is in line with the previously reported in *S. aurata* along larval development (Koumoundouros et al., 1997b), indicative of the reduced viability of larvae showing this type of skeletal anomaly.

In the present study, vertebral deformities (compression, fusion and/or displacement) were also reported, mainly in the haemal region (Hv1–3). The deformities in these vertebrae seemed to be related to a high incidence of lordosis in early juveniles (71 dph). Pre-haemal lordosis and kyphosis and haemal vertebra compression and fusion deformities are also severe deformities found to reduce larval survival in marine fish species (Koumoundouros et al., 2002; Kranenborg et al., 2005; Sfakianakis et al., 2006; Fernández et al., 2008; Ortiz-Delgado et al., 2014). These deformities may result from an increased mechanical load on the axial skeleton due to either high water speed in rearing tanks (Kranenborg et al., 2005) and/or the lack of a functional swim bladder (Chatain, 1994; Kitajima, 1979; Nagano et al., 2007; Tsuji et al., 2016). The last causative factor seems to be the most probable hypothesis in our samples, where 40% of the larvae at 25 dph do not show inflated swim bladder. Histological analysis in *P. oxygeneios* showed as inflation of the swim bladder occurs at 10 dph and was suggested to not be related with

exogenous feeding (Anderson et al., 2012). Similarly, in wreckfish larvae swim bladder inflation occurred earlier than exogenous feeding starts (at 7 dph).

Finally, most common skeletal deformities in the caudal fin complex are considered non-severe deformities (Koumoundouros, 2010) and perhaps, since it is the last region to complete skeletogenesis in most of the studied species (Fernández and Gisbert, 2010), it is the one more prone to show anomalies. In our case, all skeletal elements composing caudal fin complex showed deformities unless the hypural 5, being the highest incidence (60%) recorded at the neural arch.

4.2. The effect of temperature and light intensity during early development

4.2.1. Curved lower jaw is not related with rearing temperature

As poikilotherm species, fish development is highly dependent on the water temperature. Indeed, a comparison of different incubation temperatures (12, 13.5, 15 and 16.5 °C) demonstrated that hapuku wreckfish showed a faster development when increasing the water temperature, although no differences in survival or length at age (at the same degree hours post fertilization) were reported (Anderson et al., 2012). Nevertheless, although no specific staining was performed, authors reported a trend of increasing deformities with increasing temperature, with 13.5 °C as the preferred incubation temperature (Anderson et al., 2012). Indeed, water temperature was previously reported to have a clear effect on skeletal malformations (Georgakopoulou et al., 2010; Boglione et al., 2013a), and particularly in jaw deformities (Okamura et al., 2007; Nagano et al., 2007). Specifically, higher rates of open jaw deformity (the same deformity phenotype here reported in wreckfish larvae) were found when *Anguilla japonica* embryos were incubated in lower water temperature (Okamura et al., 2007). In order to explore when this type of deformity was related with the water temperature during early development of wreckfish, we compared the incidence of this deformity when embryos and larvae were incubated and reared at 13 or 16 °C until 7 dph. In our case, no significant differences in the incidence of jaw deformities were found when these two temperatures were used. These results suggest that, in this fish species, initial egg quality and/or another abiotic factor might be the main causative factor of this skeletal deformity rather than rearing temperature during early development.

4.2.2. Light intensity is associated to larval survival

Visual system development, including eye development, is genetically determined but it can be also environmentally triggered/modified by light conditions (Wang et al., 2021). Indeed, determined and species-specific light/dark cycles, light intensity and spectrum conditions are needed to fish display their natural behavior and proper larval development (Villamizar et al., 2009, 2011). Particular light conditions during larval development are required to identify live preys, which

efficiency is crucial during the endogenous to exogenous nutrition (Evans and Browman, 2004; Yoseda et al., 2008; Villamizar et al., 2011). Light intensity at water surface can affect the efficiency with which a larvae can capture the preys and therefore, the larval survival (Yoseda et al., 2008). In the present study, wreckfish larval survival rate was lower when reared at 600 lx at water surface, suggesting a minimum light intensity is required to succeed in first feeding, immediately after they have exhausted the endogenous reserves. This is in line with previous reports in similar species. For instance, coral grouper (*Plectropomus leopardus*) larvae reared at 0 lx exhibited stagnant and/or negative growth, while increased light intensity significantly improved larval feeding efficiency, growth, and survival (Yoseda et al., 2008). However, although the effect of light on the appearance of skeletal deformities have been already demonstrated, inducing jaw deformities in *Solea senegalensis* larvae (Blanco-Vives et al., 2010), the higher incidence of curved lower jaw with increased light intensities here reported might not be directly and/or exclusively associated with light intensity, as using the proper light intensity in the standard protocol also led to a high frequency of this deformity. Most likely, the higher incidence of this (and other skeletal deformities) present in larvae reared with light intensities higher than 600 lx might be due to the greater chances to capture live feed (increasing their survival), rather than being its origin.

5. Conclusions

The present study described the variability on the fertilization, hatching and survival rate of larvae produced by a wild wreckfish broodstock maintained in captivity, which are the main bottlenecks for the industrial farming of this species. The basic knowledge on the normal osteological development here reported is essential as a reference data for future experiments to improve larval survival and quality. Curved jaw deformity and lordosis seemed to be the most severe deformities, partially explaining the low wreckfish larval survival. Light intensity at water surface affected larval survival, and larvae reared at higher light intensity than 900 lx showed an increased incidence of jaw deformities at 21 dph. Despite that there is still a long path until reaching minimum hatching and survival rates to allow wreckfish industrial farming, fundamental information gained from this study will certainly contribute to made relevant improvements, including the prevention of skeletal deformities.

Funding

This work was partially funded by the NEWSPEC project Unión Europea a través del Fondo Europeo Marítimo y de Pesca (FEMP). M.C., P.N., and I.F. thanks the support from the network LARVAplus “Estrategias de desarrollo y mejora de la producción de larvas de peces en Iberoamerica” (117RT0521) funded by the Programa Iberoamericano de Ciencia y Tecnología para el Desarrollo (CYTED).

Supplementary data to this article can be found online at <https://doi.org/10.1016/j.aquaculture.2023.739935>.

Author contributions

Amin Mokhles Abadi Farahani: formal analysis, writing—original draft preparation, writing—review and editing; **Maximo Coronado:** formal analysis, writing—review and editing; **Santiago Bragado:** formal analysis; **Maria José Justo:** formal analysis; **Xoana Blanco:** formal analysis; **Aitor Sotelo:** formal analysis; **Paola Navarrete:** formal analysis, writing—review and editing; **Blanca Álvarez-Blázquez:** Conceptualization, methodology, formal analysis, writing—review and editing; **Ignacio Fernández:** Conceptualization, methodology, formal analysis, writing—original draft preparation, writing—review and editing.

Declaration of Competing Interest

The authors declare to possess no competing interests.

Data availability

Data will be made available on request.

Acknowledgements

B. A. and I.F. acknowledge the excellent technical work of Gloria Cordeiro, Ernesto Casal, Diego Vicenzutto, Pablo Ibañez, Carlos Santaló and Pedro Reguera from the Centro Tecnológico Naval during the experimental trial.

References

- Amoroso, G., Adams, M.B., Ventura, T., Carter, C.G., Cobcroft, J.M., 2016a. Skeletal anomaly assessment in diploid and triploid juvenile Atlantic salmon (*Salmo salar* L.) and the effect of temperature in freshwater. *J. Fish Dis.* 39 (4), 449–466. <https://doi.org/10.1111/jfd.12438>.
- Amoroso, G., Ventura, T., Cobcroft, J.M., Adams, M.B., Elizur, A., Carter, C.G., 2016b. Multigenic delineation of lower jaw deformity in triploid Atlantic salmon (*Salmo salar* L.). *PLoS One* 11 (12), e0168454. <https://doi.org/10.1371/journal.pone.0168454>.
- Barahona-Fernandes, M.H., 1982. Body deformation in hatchery reared european sea bass *Dicentrarchus labrax* (L). Types, prevalence and effect on fish survival. *J. Fish Biol.* 21 (3), 239–249. <https://doi.org/10.1111/j.10958649.1982.tb02830.x>.
- Bird, N.C., Mabee, P.M., 2003. Developmental morphology of the axial skeleton of the zebrafish, *Danio rerio* (Ostariophysi: Cyprinidae). *Dev. Dyn.* 228 (3), 337–357. <https://doi.org/10.1002/dvdy.10387>.
- Blanco-Vives, B., Villamizar, N., Ramos, J., Bayarri, M.J., Chereguini, O., Sánchez-Vázquez, F.J., 2010. Effect of daily thermo-and photo-cycles of different light spectrum on the development of Senegal sole (*Solea senegalensis*) larvae. *Aquaculture* 306 (1–4), 137–145. <https://doi.org/10.1016/j.aquaculture.2010.05.034>.
- Boeuf, G., Le Bail, P.-Y., 1999. Does light have an influence on fish growth? *Aquaculture* 177, 129–152.
- Boglione, C., Gagliardi, F., Scardi, M., Cataudella, S., 2001. Skeletal descriptors and quality assessment in larvae and post-larvae of wild-caught and hatchery reared gilthead sea bream (*Sparus aurata* L. 1758). *Aquaculture* 192 (1), 1–22. [https://doi.org/10.1016/S0044-8486\(00\)00446-4](https://doi.org/10.1016/S0044-8486(00)00446-4).
- Boglione, C., Gisbert, E., Gavaia, P., Witten, P.E., Moren, M., Fontagné, S., Koumoundouros, G., 2013a. Skeletal anomalies in reared european fish larvae and juveniles. Part 2: Main typologies, occurrences and causative factors. *Rev. Aquac.* 5 (1), 121–167. <https://doi.org/10.1111/raq.12016>.
- Boglione, C., Gavaia, P., Koumoundouros, G., Gisbert, E., Moren, M., Fontagné, S., Witten, P.E., 2013b. Skeletal anomalies in reared european fish larvae and juveniles. Part 1: normal and anomalous skeletogenic processes. *Rev. Aquac.* 5 (1), 99–120. <https://doi.org/10.1111/raq.12015>.
- Brzuzan, P., Woźny, M., Dobosz, S., Kuźmiński, H., Łuczniński, M.K., Góra, M., 2007. Blue sac disease in larval whitefish, *Coregonus lavaretus* (L.): pathological changes in mRNA levels of cyp1a, era, and p53. *J. Fish Dis.* 30 (3), 169–173. <https://doi.org/10.1111/j.13652761.2007.00784.x>.
- Chatain, B., 1994. Abnormal swimbladder development and lordosis in sea bass (*Dicentrarchus labrax*) and sea bream (*Sparus aurata*). *Aquaculture* 119 (4), 371–379. [https://doi.org/10.1016/0044-8486\(94\)90301-8](https://doi.org/10.1016/0044-8486(94)90301-8).
- Cobcroft, J.M., Pankhurst, P.M., Sadler, J., Hart, P.R., 2001. Jaw development and malformation in cultured striped trumpeter *Latris lineata*. *Aquaculture* 199 (3–4), 267–282. [https://doi.org/10.1016/S0044-8486\(01\)00592-0](https://doi.org/10.1016/S0044-8486(01)00592-0).
- Collette, B., Fernandes, P., Heessen, H., Smith-Vaniz, W.F., 2015. *Polyprion americanus* (Europe assessment). The IUCN Red List of Threatened Species 2015: e.T43972A45795607. Accessed on 12 December 2022.
- Cordova-de la Cruz, S.E., Riesco, M.F., Martínez-Bautista, G., Calzada-Ruiz, D., Martínez-Burguete, T., Peña-Marín, E.S., Álvarez-Gonzalez, C.A., Fernández, I., 2022. Larval development in tropical gar (*Atractosteus tropicus*) is dependent on the embryonic thermal regime: ecological implications under a climate change context. *Fishes* 7, 16. <https://doi.org/10.3390/fishes7010016>.
- Cubbage, C.C., Mabee, P.M., 1996. Development of the cranium and paired fins in the zebrafish *Danio rerio* (Ostariophysi, Cyprinidae). *J. Morphol.* 229 (2), 121–160. [https://doi.org/10.1002/\(SICI\)10976744687\(199608\)229:2%3C121::AIDJMOR1%3E3.0.CO;2-4](https://doi.org/10.1002/(SICI)10976744687(199608)229:2%3C121::AIDJMOR1%3E3.0.CO;2-4).
- Daoulas, C., Economou, A.N., Bantavas, I., 1991. Osteological abnormalities in laboratory reared sea-bass (*Dicentrarchus labrax*) fingerlings. *Aquaculture* 97 (2–3), 169–180. [https://doi.org/10.1016/0044-8486\(91\)90263-7](https://doi.org/10.1016/0044-8486(91)90263-7).
- de Azevedo, A.M., Losada, A.P., Barreiro, A., Barreiro, J.D., Ferreiro, I., Riaza, A., Vázquez, S., Quiroga, M.I., 2017. Skeletal anomalies in reared Senegalese sole *Solea senegalensis* juveniles: a radiographic approach. *Dis. Aquat. Org.* 124, 117–129. <https://doi.org/10.3354/dao03110>.
- Deudero, S., Morales-Nin, B., 2000. Occurrence of *Polyprion americanus* under floating objects in western Mediterranean oceanic waters, inference from stomach contents

- analysis. *J. Mar. Biol. Assoc. U. K.* 80 (4), 751–752. <https://doi.org/10.1017/S0025315400002666>.
- Dionísio, G., Campos, C., Valente, L.M.P., Conceição, L.E.C., Cancela, M.L., Gavaia, P.J., 2012. Effect of egg incubation temperature on the occurrence of skeletal deformities in *Solea senegalensis*. *J. Appl. Ichthyol.* 28, 471–476.
- Evans, B.I., Browman, H.I., 2004. Variation in the development of the fish retina. *Am. Fish. Soc. Symp.* 40, 145–166.
- Faustino, M., Power, D.M., 1998. Development of osteological structures in the sea bream: vertebral column and caudal fin complex. *J. Fish Biol.* 52 (1), 11–22. <https://doi.org/10.1111/j.1095-8649.1998.tb01548.x>.
- Faustino, M., Power, D.M., 1999. Development of the pectoral, pelvic, dorsal and anal fins in cultured sea bream. *J. Fish Biol.* 54 (5), 1094–1110. <https://doi.org/10.1111/689.j.1095-8649.1999.tb00860.x>.
- Faustino, M., Power, D.M., 2001. Osteologic development of the viscerocranial skeleton in sea bream: alternative ossification strategies in teleost fish. *J. Fish Biol.* 58 (2), 537–572. <https://doi.org/10.1006/jfbi.2000.1474>.
- Fernández, I., Gisbert, E., 2010. Senegalese sole bone tissue originated from chondral ossification is more sensitive than dermal bone to high vitamin A content in enriched *Artemia*. *J. Appl. Ichthyol.* 26 (2), 344–349.
- Fernández, I., Gisbert, E., 2011. The effect of vitamin A on flatfish development and skeletogenesis: A review. *Aquaculture* 315 (1–2), 34–48. <https://doi.org/10.1016/j.aquaculture.2010.11.025>.
- Fernández, I., Granadeiro, L., Darias, M.J., Gavaia, P.J., Andree, K.B., Gisbert, E., 2018. *Solea senegalensis* skeletal ossification and gene expression patterns during metamorphosis: new clues on the onset of skeletal deformities during larval to juvenile transition. *Aquaculture* 496, 153–165. <https://doi.org/10.1016/j.aquaculture.2018.07.022>.
- Fernández, I., Hontoria, Francisco, Ortiz-Delgado, Juan B., Kotzamanis, Yannis, Estévez, Alicia, Zambonino-Infante, Jose Luis, Gisbert, Enric, 2008. Larval performance and skeletal deformities in farmed gilthead sea bream (*Sparus aurata*) fed with graded levels of Vitamin A enriched rotifers (*Brachionus plicatilis*). *Aquaculture* 283 (1–4), 102–115. <https://doi.org/10.1016/j.aquaculture.2008.06.037>.
- Fernández, I., Toledo-Solís, F.J., Tomás-Almenar, C., Larrán, A.M., Cárdbaba, P., Laguna, L.M., Sanz Galán, M., Mateo, J.A., 2021. Skeletal development and deformities in tench (*Tinca tinca*): from basic knowledge to regular monitoring procedure. *Animals* 11 (3), 621. <https://doi.org/10.3390/ani11030621>.
- Fjellidal, P.A., Hansen, T.J., Lock, E.J., Wargelius, A., Fraser, T.W.K., Sambrabus, F., El-Mowafi, A., Albrektsen, S., Waagbø, R., Ørnstrud, R., 2016. Increased dietary phosphorus prevents vertebral deformities in triploid atlantic salmon (*Salmo salar* L.). *Aquac. Nutr.* 22 (1), 72–90. <https://doi.org/10.1111/anu.12238>.
- Fuiman, L.A., Poling, K.R., Higgs, D.M., 1998. Quantifying developmental progress for comparative studies of larval fishes. *Oecologia* 3, 602–611. <https://doi.org/10.2307/1447790>.
- Georgakopoulou, E., Katharios, P., Divanach, P., Koumoundouros, G., 2010. Effect of temperature on the development of skeletal deformities in gilthead seabream (*Sparus aurata* Linnaeus, 1758). *Aquaculture* 308 (1–2), 13–19. <https://doi.org/10.1016/j.aquaculture.2010.08.006>.
- Gunasekera, R.M., Gooley, G.J., De Silva, S.S., 1998. Characterisation of “swollen yolk-sac syndrome” in the Australian freshwater fish murray cod, *Maccullochella peelii pealii*, and associated nutritional implications for large scale aquaculture. *Aquaculture* 169 (1–2), 69–85. [https://doi.org/10.1016/S0044-8486\(98\)00371-8](https://doi.org/10.1016/S0044-8486(98)00371-8).
- Haga, Y., Takeuchi, T., Seikai, T., 2002. Influence of all-trans retinoic acid on pigmentation and skeletal formation in larval Japanese flounder. *Fish. Sci.* 68 (3), 560–570. <https://doi.org/10.1046/j.1444-2906.2002.00462.x>.
- Houde, E.D., Potthoff, T., 1976. Egg and larval development of the sea bream *Archosargus rhomboidalis* (Linnaeus): pisces, sparidae. *Bull. Mar. Sci.* 26 (4), 506–529.
- Kitajima, C., 1979. Swim bladder deformity and lordosis in hatchery-reared black sea bream, *Acanthopagrus schlegelii*. *Bull. Nagasaki Prefect. Inst. Fish. (Japan)* 5, 27–35.
- Kohn, Yair Y., Symonds, Jane E., 2012. Evaluation of egg quality parameters as predictors of hatching success and early larval survival in hapuku (*Polyprion oxygeneios*). *Aquaculture* 342–343, 42–47. <https://doi.org/10.1016/j.aquaculture.2012.02.014>.
- Koumoundouros, G., 2010. Morpho-anatomical abnormalities 745 in Mediterranean marine aquaculture. In: Koumoundouros, G. (Ed.), *Recent Advances in Aquaculture Research*. Kerala, Transworld Research Network, pp. 125–148.
- Koumoundouros, G., Gagliardi, F., Divanach, P., Boglione, C., Cataudella, S., Kentouri, M., 1997a. Normal and abnormal osteological development of caudal fin in *Sparus aurata* L. fry. *Aquaculture* 149 (3–4), 215–226. [https://doi.org/10.1016/S0044-8486\(96\)01443-3](https://doi.org/10.1016/S0044-8486(96)01443-3).
- Koumoundouros, G., Oran, G., Divanach, P., Stefanakis, S., Kentouri, M., 1997b. The opercular complex deformity in intensive gilthead sea bream (*Sparus aurata* L.) larviculture. Moment of apparition and description. *Aquaculture* 156 (1–2), 165–177. [https://doi.org/10.1016/S0044-8486\(97\)89294-0](https://doi.org/10.1016/S0044-8486(97)89294-0).
- Koumoundouros, G., Maingot, E., Divanach, P., Kentouri, M., 2002. Kyphosis in reared sea bass (*Dicentrarchus labrax* L.): ontogeny and effects on mortality. *Aquaculture* 209 (1–4), 49–58. [https://doi.org/10.1016/S0044-8486\(01\)00821-3](https://doi.org/10.1016/S0044-8486(01)00821-3).
- Koumoundouros, G., Gisbert, E., Fernández, I., Cabrera, E., Galindo-Villegas, J., Conceição, L., 2017. Quality descriptors and predictors in farmed marine fish larvae and juveniles. In: LEC, Conceição, Tandler, A. (Eds.), *Success Factors for Fish Larval Production*. John Wiley & Sons, Oxford, UK, pp. 443–463. ISBN: 978-1-119-07216-4.
- Kranenborg, S., Waarsing, J.H., Muller, M., Weinans, H., van Leeuwen, J.L., 2005. Lordotic vertebrae in sea bass (*Dicentrarchus labrax* L.) are adapted to increased loads. *J. Biomech.* 38 (6), 1239–1246. <https://doi.org/10.1016/j.jbiomech.2004.06.011>.
- Kusaka, A., Yamaoka, K., Yamada, T., Abe, M., 1994. Development of caudal skeleton of the red-spotted grouper, *Epinephelus akaara*. *Aquac. Sci.* 42 (2), 273–278. <https://doi.org/10.1123/aquaculturesci.1953.42.273>.
- Lewis, L.M., Lall, S.P., 2006. Development of the axial skeleton and skeletal abnormalities of Atlantic halibut (*Hippoglossus hippoglossus*) from first feeding through metamorphosis. *Aquaculture* 257 (1–4), 124–135. <https://doi.org/10.1016/j.aquaculture.2006.02.067>.
- Lijalad, M., Powell, M.D., 2009. Effects of lower jaw deformity on swimming performance and recovery from exhaustive exercise in triploid and diploid Atlantic salmon *Salmo salar* L. *Aquaculture* 290 (1–2), 145–154. <https://doi.org/10.1016/j.aquaculture.2009.01.039>.
- Linares, F., Pérez Rial, E., Rodriguez, J.L., Pazos, G., Álvarez-Blázquez, B., 2021. Biometric parameters and biochemical composition of wild wreckfish (*Polyprion americanus*). *Mar. Biol. Res.* 17 (3), 234–246. <https://doi.org/10.1080/17451000.2021.1923752>.
- McMenamin, Sarah K., Parichy, David M., 2013. Chapter Five - Metamorphosis in Teleosts. *Curr. Top. Dev. Biol.* 103, 127–165.
- Nagano, N., Hozawa, A., Fujiki, W., Yamada, T., Miyaki, K., Sakakura, Y., Hagiwara, A., 2007. Skeletal development and deformities in cultured larval and juvenile seven-band grouper, *Epinephelus septemfasciatus* (Thunberg). *Aquac. Res.* 38 (2), 121–130. <https://doi.org/10.1111/j.1365-2109.2006.01627.x>.
- Okamura, A., Yamada, Y., Horie, N., et al., 2007. Effects of water temperature on early development of Japanese eel *Anguilla japonica*. *Fish. Sci.* 73, 1241–1248. <https://doi.org/10.1111/j.1444-2906.2007.01461.x>.
- Ortiz-Delgado, J.B., Fernández, I., Sarasquete, C., Gisbert, E., 2014. Normal and histopathological organization of the opercular bone and vertebrae in gilthead sea bream *Sparus aurata*. *Aquat. Biol.* 21 (1), 67–84. <https://doi.org/10.3354/ab00568>.
- Papadaki, M., Peleteiro, J.B., Alvarez-Blázquez, B., Rodríguez Villanueva, J.L., Linares, F., Vilar, A., Pérez Rial, E., Lluç, N., Fakriadis, I., Sigelaki, I., Mylonas, C.C., 2018. Description of the annual reproductive cycle of wreckfish *Polyprion americanus* in captivity. *Fishes* 3 (4), 1–20. <https://doi.org/10.3390/fishes3040043>.
- Papandroulakis, N., Suquet, M., Spedicato, M.T., Machias, A., Fauvel, C., Divanach, P., 2004. Feeding rates, growth performance and gametogenesis of wreckfish (*Polyprion americanus*) kept in captivity. *Aquat. Int.* 12 (4–5), 395–407. <https://doi.org/10.1023/B:AQU.0000042133.69455.95>.
- Papandroulakis, N., Mylonas, C.C., Syggelaki, E., Katharios, P., Divanach, P., 2008. First reproduction of captive-reared wreckfish (*Polyprion americanus*) using GnRH implants. *Aquat. Europe* 08 (8), 15–18.
- Percie du Sert, N., Hurst, V., Ahluwalia, A., Alam, S., Avey, M.T., Baker, M., Browne, W. J., Clark, A., Cuthill, I.C., Dirnagl, U., Emerson, M., 2020. The arrive guidelines 2.0: updated guidelines for reporting animal research. *J. Cereb. Blood Flow Metab.* 4 (9), 1769–1777. <https://doi.org/10.1136/bmjso-2020-100115>.
- Peres, M.B., Klippel, S., 2003. Reproductive biology of southwestern Atlantic wreckfish, *Polyprion americanus* (Teleostei: Polyprionidae). *Environ. Biol. Fish* 68 (2), 163–173. <https://doi.org/10.1023/B:EBFI.0000003845.43700.29>.
- Pérez, E., Linares, F., Rodríguez Villanueva, J.L., Vilar, A., Mylonas, C.C., Fakriadis, I., Papadaki, M., Papandroulakis, N., Papadakis, I., Robles, R., Fauvel, C., 2019. Wreckfish (*Polyprion americanus*). New knowledge about reproduction, larval husbandry, and nutrition. Promise as a new species for aquaculture. *Fishes* 4 (1). <https://doi.org/10.3390/fishes4010014>.
- Polo, A., Yúfera, M., Pascual, E., 1991. Effects of temperature on egg and larval development of *Sparus aurata* L. *Aquaculture* 92, 367–375. [https://doi.org/10.1016/0044-8486\(91\)90042-6](https://doi.org/10.1016/0044-8486(91)90042-6).
- Quémener, L., Suquet, M., Mero, D., Gaignon, J.-L., 2002. Selection method of new candidates for finfish aquaculture: the case of the french Atlantic, the channel and the north sea coasts. *Aquat. Living Resour.* 15 (5), 293–302. [https://doi.org/10.1016/S0990-7440\(02\)01187-7](https://doi.org/10.1016/S0990-7440(02)01187-7).
- Richards, W.J., Miller, R.V., Houde, E.D., 1974. Egg and larval development of the Atlantic thread herring, *opisthonema oglinum*. *Fish. Bull.* 72 (4), 1123–1136. Retrieved from <http://serfc/fish-larval-reprints>.
- Ruchin, A.B., 2021. Effect of illumination on fish and amphibian: development, growth, physiological and biochemical processes. *Rev. Aquac.* 13, 567–600. [https://doi.org/10.1016/S0990-7440\(02\)01187-7](https://doi.org/10.1016/S0990-7440(02)01187-7).
- Sadler, J., Pankhurst, P.M., King, H.R., 2001. High prevalence of skeletal deformity and reduced gill surface area in triploid Atlantic salmon (*Salmo salar* L.). *Aquaculture* 198 (3–4), 369–386. [https://doi.org/10.1016/S00448486\(01\)00508-7](https://doi.org/10.1016/S00448486(01)00508-7).
- Sedberry, G.R., Andrade, C.A.P., Carlin, J.L., Chapman, R.W., Luckhurst, B.E., Manooch III, C.S., Menezes, G., Thomsen, B., Ulrich, G.F., 1999. Wreckfish *Polyprion americanus* in the North Atlantic: fisheries, biology, and long-lived fish. *Am. Fish. Soc. Symp.* 23, 27–50.
- Seoka, M., Yamada, S., Iwata, Y., Yanagisawa, T., Nakagawa, T., Kumai, H., 2003. Differences in the biochemical content of buoyant and non-buoyant eggs of the Japanese eel, *Anguilla japonica*. *Aquaculture* 216 (1–4), 355–362. [https://doi.org/10.1016/S0044-8486\(02\)00459-3](https://doi.org/10.1016/S0044-8486(02)00459-3).
- Sfakianakis, D.G., Doxa, C.K., Kouttouki, S., Koumoundouros, G., Maingot, E., Divanach, P., Kentouri, M., 2005. Osteological development of the vertebral column and of the fins in *Diplodus puntazzo* (Cetti, 1777). *Aquaculture* 250 (1–2), 36–46. <https://doi.org/10.1016/j.aquaculture.2005.03.042>.
- Sfakianakis, D.G., Georgakopoulou, E., Papadakis, I.E., Divanach, P., Kentouri, M., Koumoundouros, G., 2006. Environmental determinants of haemal lordosis in European sea bass, *Dicentrarchus labrax* (Linnaeus, 1758). *Aquaculture* 254 (1–4), 54–64. <https://doi.org/10.1016/j.aquaculture.2005.10.028>.
- Symonds, J.E., Walker, S.P., Pether, S., Gublin, Y., McQueen, D., King, A., Irvine, G.W., Setiawan, A.N., Forsythe, J.A., Bruce, M., 2014. Developing yellowtail kingfish (*Seriola lalandi*) and hapuku (*Polyprion oxygeneios*) for New Zealand aquaculture. *N. Z. J. Mar. Freshw. Res.* 48 (3), 371–384. <https://doi.org/10.1080/00288330.2014.930050>.

- Taylor, Matthew D., Chick, Rowan C., Kai, Lorenzen, Ann-Lisbeth, Agnalt, Kenneth, M. Leber, Blankenship, H. Lee, Vander Haegen, Geraldine, Loneragan, Neil R., 2017. Fisheries enhancement and restoration in a changing world. *Fisheries Res.* 186, 407–412. <https://doi.org/10.1016/j.fishres.2016.10.004>.
- Tsuji, M., Uji, S., Tsuchihashi, Y., Okada, K., Kawamura, T., Katoh, T., Kasuya, T., Nigo, T., Hamabe, A., Miyamoto, A., Nakamura, S., 2016. Promotion of initial swim bladder inflation and effect of initial inflation failure on skeletal malformation in cultured seven-band grouper *Hyporhamphus septemfasciatus* (Thunberg). *Aquac. Res.* 47 (6), 1954–1971. <https://doi.org/10.1111/are.12652>.
- Verhaegen, Y., Adriaens, D., De Wolf, T., Dhert, P., Sorgeloos, P., 2007. Deformities in larval gilthead sea bream (*Sparus aurata*): a qualitative and quantitative analysis using geometric morphometrics. *Aquaculture* 268 (1–4), 156–168. <https://doi.org/10.1016/j.aquaculture.2007.04.037>.
- Villamizar, N., García-Alcazar, A., Sánchez-Vázquez, F.J., 2009. Effect of light spectrum and photoperiod on the growth, development and survival of European sea bass (*Dicentrarchus labrax*) larvae. *Aquaculture* 292 (1–2), 80–86. <https://doi.org/10.1016/j.aquaculture.2009.03.045>.
- Villamizar, N., Blanco-Vives, B., Migaud, H., Davie, A., Carboni, S., Sanchez-Vazquez, F. J., 2011. Effects of light during early larval development of some aquacultured teleosts: A review. *Aquaculture* 315 (1–2), 86–94. <https://doi.org/10.1016/j.aquaculture.2010.10.036>.
- Wakefield, C.B., Newman, S.J., Boddington, D.K., 2013. Exceptional longevity, slow growth and late maturation infer high inherent vulnerability to exploitation for bass grouper *Polyprion americanus* (Teleostei: Polyprionidae). *Aquat. Biol.* 18 (2), 161–174. <https://doi.org/10.3354/ab00501>.
- Wang, Y., Zhou, L., Wu, L., et al., 2021. Evolutionary ecology of the visual opsin gene sequence and its expression in turbot (*Scophthalmus maximus*). *BMC Ecol. Evo.* 21, 114. <https://doi.org/10.1186/s12862-021-01837-2>.
- Wargelius, A., Fjellidal, P.G., Hansen, T., 2005. Heat shock during early somitogenesis induces caudal vertebral column defects in Atlantic salmon (*Salmo salar*). *Dev. Genes Evol.* 215, 350–357.
- Yoseda, K., Yamamoto, K., Asami, K., Chimura, M., Hashimoto, K., Kosaka, S., 2008. Influence of light intensity on feeding, growth, and early survival of leopard coral grouper (*Plectropomus leopardus*) larvae under mass-scale rearing conditions. *Aquaculture* 279 (1–4), 55–62. <https://doi.org/10.1016/j.aquaculture.2008.04.002>.
- Huntingford, F.A., 2004. Implications of domestication and rearing conditions for the behaviour of cultivated fishes. *J. Fish Biol.* 65 (S1), 122–142. <https://doi.org/10.1111/j.0022-1112.2004.00562.x>.
- Matsuoka, Masanobu, 1982. Development of Vertebral Column and Caudal Skeleton of the Red Sea Bream, *Pagrus major*. *Jpn. J. Ichthyol.* 29 (2). https://www.jstage.jst.go.jp/article/jji1950/29/3/29_3_285/_pdf.
- Matusse, R.D. Nédia, Alfonso, Pita, Montse, Peréz, Trucco, M. Inés, José, Benito Peleteiro, Pablo, Presa, 2016. First-generation genetic drift and inbreeding risk in hatchery stocks of the wreckfish *Polyprion americanus*. *Aquaculture* 451, 125–136.
- Anderson, S.A., Salinas, I., Walker, S.P., Gublin, Y., Pether, S., Kohn, Y.Y., Symonds, J.E., 2012. Early development of New Zealand hapuku *Polyprion oxygeneios* eggs and larvae. *J. Fish Biol.* 80 (3), 555–571. <https://doi.org/10.1111/j.1095-8649.2011.03191.x>.